



Journal of Mining and Environment (JME)

journal homepage: www.jme.shahroodut.ac.ir



Stability Analysis of Block-Flexural Toppling of Rock Blocks with Round Edges

Hassan Sarfaraz*

School of Mining Engineering, College of Engineering, University of Tehran, Tehran, Iran

Article Info

Received 2 October 2020

Received in Revised form 21 November 2020

Accepted 25 November 2020

Published online 25 November 2020

[DOI:10.22044/jme.2020.10128.1951](https://doi.org/10.22044/jme.2020.10128.1951)

Keywords

Rock Slope Stability

Spheroidal Weathering

Round Edges

Theoretical Solution

Abstract

One of the most conventional toppling instabilities is the block-flexural toppling failure that occurs in civil and mining engineering projects. In this kind of failure, some rock columns are broken due to tensile bending stresses, and the others are overturned due to their weights, and finally, all of the blocks topple together. A specific feature of spheroidal weathering is the rounding of the rock column edges. In the mode of flexural toppling failure, rounding of edges happens only at the upper corners of the block but in the block toppling failure mode, due to the presence of cross-joints at the base of the block, rounding of edges also occurs at the base of the block. In this work, a theoretical model is offered to block-flexural toppling failure regarding the erosion phenomenon. The suggested methodology is evaluated through a typical example and a case study. The results of this research work illustrate that in the stable slopes with rectangular prismatic blocks, where the safety factor value is close to one, the slope is subjected to failure due to erosion. Also the results obtained show that the recommended approach is conservative in analyzing the block-flexural toppling failure, and this approach can be applied to evaluate this failure.

1. Introduction

Ashby [1] has examined the overturning of rock blocks, recommending principles based on the theoretical technique and physical models. After two years, some experimental models were carried out by Erguvanli and Goodman [2] to investigate the toppling failure. The toppling failures have been categorized into the primary and secondary kinds [3]. In the main toppling failure kinds, the

critical reason for instability is the rock block weight (Figure 1). The secondary toppling instabilities have been stimulated through some external factors, and many types have been evaluated through the analytical method, and the physical and numerical modelling for these failures [4-12].

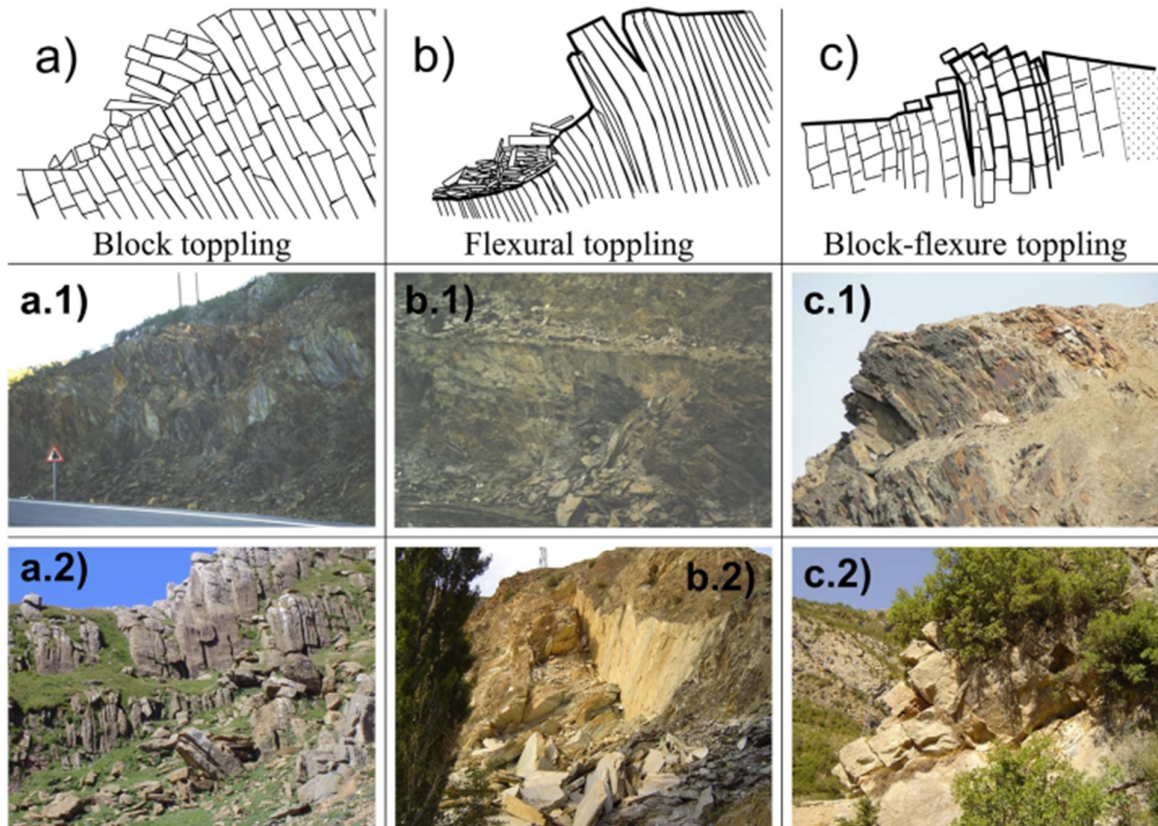


Figure 1. Primary toppling failure (a: blocky, b: flexural, and c: block-flexural toppling failure) [13].

Based on the Goodman and Bray's category, some studies have been published by the theoretical approaches, and the experimental and numerical models [14-16]. Adhikary and Dyskin [17] have performed the centrifugal model for the flexural toppling failure. A simplified methodology has been presented to analyze the flexural toppling failure on the basis of the compatibility principle of cantilever beams [18, 19]. Also Zheng *et al.* [20, 21] have recommended a new method for the analysis of this failure based on the limit equilibrium's theory. Sarfaraz [22] has proposed a new analytical methodology in order to obtain the safety factor in flexural toppling using the Sarma's method. Amini *et al.* [23] have suggested an approach for the analysis of the block-flexural toppling failure. Sarfaraz and Amini [24] have simulated this failure using the UDEC software. Some researches have studied the impact of local response on the toppling failure using physical and numerical modellings [25, 26]. Bowa and Xia [27] have examined the impact of the counter-tilted failure plane angle on the block toppling failure, and they validated their results using the 3DEC software. Alejano *et al.* [13, 28] have investigated the stability of rock column topplings with round edges based on the physical and analytical

methodologies. For the jointed rock mass defining prismatic blocks, the spheroidal weathering produces an ongoing transformation of the originally sharp-edge prismatic blocks into the blocks that display rounded edges. If the process of weathering continues indefinitely, the blocks with a spheroidal shape are produced. In this work, an analytical method is recommended for the block-flexural toppling failure in the case of rock columns with rounded edges, and then the outcomes are discussed.

2. Suggested Analytical methodology

A representation picture of the suggested theoretical method is indicated in Figure 2. The geometry and forces acting on the I^{th} and $(I+1)^{\text{th}}$ blocks are illustrated in this Figure. In order to evaluate this failure, the following two states were examined:

- Case 1: A block with the block toppling potential was located between two blocks with a flexural toppling potential.
- Case 2: A block with the flexural toppling potential was located between two blocks with a block toppling potential.

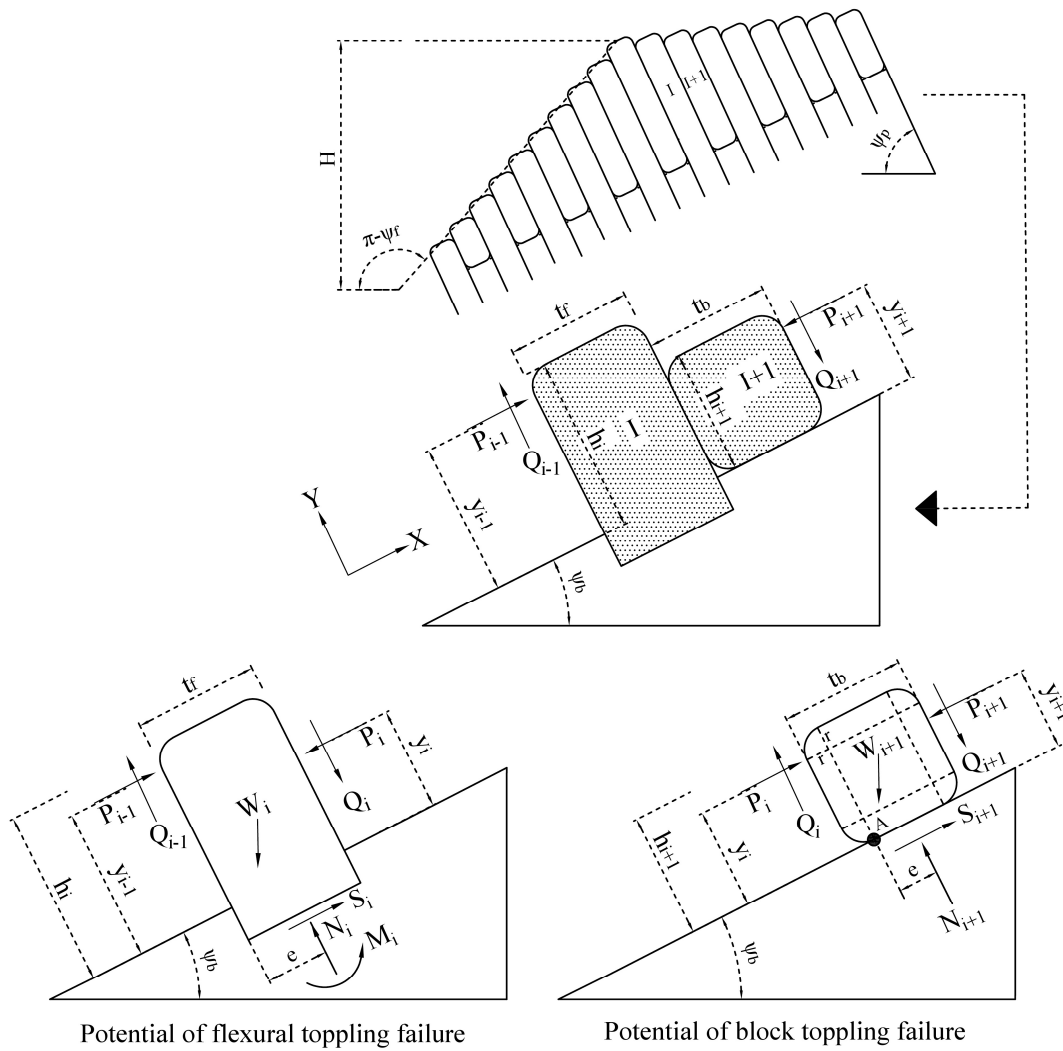


Figure 2. Schematic picture of the theoretical solution.

2.1. Analyzing of case 1

This analysis can be sub-divided into the following three types depending on whether the (I+1)th block has the prone to be toppling, sliding or stable:

- a. The (I+1)th block has the prone to toppling failure, and is stable against sliding. In this case, the following conditions occur (Figure 3):

$$Q_{i+1} = P_{i+1} \tan \varphi_c \tag{1}$$

$$Q_i = P_i \tan \varphi_c \tag{2}$$

$$e = 0 \tag{3}$$

$$y_i = h_{i+1} - r \tag{4}$$

$$y_{i+1} = 0.75(h_{i+2} - r) \tag{5}$$

$$S_{i+1} < (c_b(t_b - 2r) + N_{i+1} \tan \phi_b) \tag{6}$$

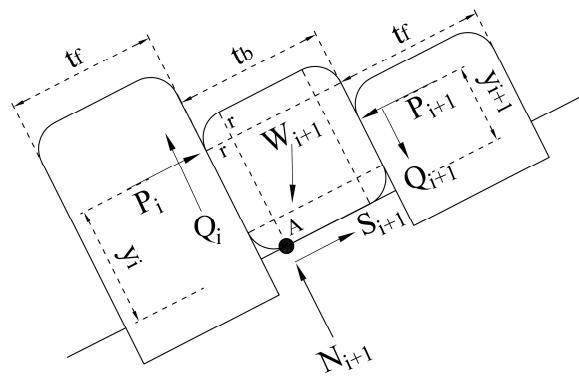


Figure 3. Analysis of three blocks with the potential of blocky and flexural toppling failures.

where:

P_i : Force of normal in inter-block

Q_i : Force of shear in inter-block

S_i : Shear force acting at the base of the block

N_i : Normal force acting at the base of the block

ϕ_c : Interface friction angle between blocks

ψ_f : Slope face angle

ψ_b : Normal dip to the discontinuities

ψ_p : Angle of discontinuities

c_b : Cohesive strength of the base of rock block

W_i : Weight force

h_i : Average block length

y_i : Application point of "P"

r : Curvature radius of block corners

H: Slope height

t: Block thickness

According to Figure 3, by considering the relationships (1) and (2), the relationship for the moment equilibrium with respect to point A can be written as follows:

$$\begin{aligned} \sum M_A = 0 \rightarrow & W_{i+1} \sin \psi_b (0.5 h_i) \\ & - W_{i+1} \cos \psi_b (0.5 t_b - r) - P_i (y_i) + P_{i+1} (y_{i+1}) \quad (7) \\ & - (P_{i+1} \tan \phi_c) (t_b - r) - P_i \tan \phi_c (r) = 0 \end{aligned}$$

The amount of force P_i can be calculated by the following equation:

$$P_{i,t} = \frac{P_{i+1} (y_{i+1} - \tan \phi_c (t_b - r) / F_s) + 0.5 W_{i+1} (\sin \psi_b h_{i+1} - \cos \psi_b (t_b - 2r))}{y_i + \tan \phi_c (r)} \quad (8)$$

- b. The (I+1)th block has the prone of sliding failure, and is stable against the blocky toppling failure, where the following conditions occur (Figure 4):

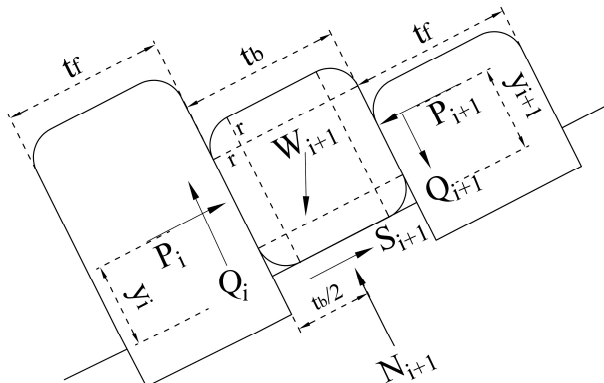


Figure 4. Analysis of three blocks with the prone of sliding and flexural toppling failures.

$$Q_{i+1} = P_{i+1} \tan \phi_c \quad (9)$$

$$Q_i = P_i \tan \phi_c \quad (10)$$

$$e = 0.5 t_b \quad (11)$$

$$y_i = 0.5 (h_{i+1} - r) \quad (12)$$

$$y_{i+1} = 0.75 (h_{i+2} - r) \quad (13)$$

$$S_{i+1} = (c_b (t_b - 2r) + N_{i+1} \tan \phi_b) \quad (14)$$

According to Figure , by writing the equilibrium equation forces:

$$S_{i+1} = P_{i+1} - P_i + W_{i+1} \sin \psi_b \quad (15)$$

$$N_{i+1} = Q_{i+1} - Q_i + W_{i+1} \cos \psi_b \quad (16)$$

with the substitution of Equation (14) into the Equations (15) and (16), the magnitude of the force P_i can be obtained as follows:

$$P_{i,S} = P_{i+1} + \frac{W_{i+1} (\sin \psi_b - \cos \psi_b \tan \phi_b / F_s) - c_b (t_b - 2r) / F_s}{1 - \tan \phi_b \tan \phi_c / F_s} \quad (17)$$

c. The (I+1)th block is stable against the sliding and toppling failure. Thus $P_i = 0$.

After examination of the above states, the force P_i is equal to $P_i = \text{Max}(P_{i,s}, P_{i,t}, 0)$.

2.2. Analyzing of case 2

This analysis can be sub-divided into the following two cases depending on whether the Ith block has the potential to be flexural toppling or shearing:

a. The Ith block has the prone for flexural toppling (Figure 5):

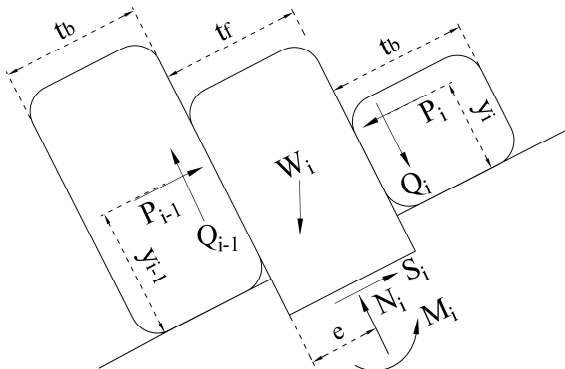


Figure 5. Analysis of three blocks with the prone of block-flexural toppling failures.

$$Q_i = P_i \tan \varphi_c \tag{18}$$

$$Q_{i-1} = P_{i-1} \tan \varphi_c \tag{19}$$

$$e = 0.5t_f \tag{20}$$

$$y_{i-1} = 0.75(h_i - r) \tag{21}$$

According to Figure 5, by writing the equilibrium equation for this block, M_i and N_i at the middle block base can be obtained by the following equation:

$$\sum F_N = 0 \rightarrow N_i = W_i \cos \psi_b \tag{22}$$

$$+P_i \tan \varphi_c - P_{i-1} \tan \varphi_c$$

$$\sum M = 0 \rightarrow M_i = P_i(y_i - 0.5 \tan \varphi_c t_f) \tag{23}$$

$$-P_{i-1}(y_{i-1} + 0.5 \tan \varphi_c t_f) + 0.5W_i h_i \sin \psi_b$$

At the block base, the maximum tensile stress can be calculated as follows:

$$\sigma_i^{y=t_f/2} = \frac{0.5M t_f}{I} - \frac{N}{t_f} \rightarrow M = \frac{2I}{t_f} \left(\sigma_i + \frac{N}{t_f} \right) \tag{24}$$

By substituting M_i and N_i from Equations (22) and (23) into Equation (24), P_{i-1} is determined:

$$P_{i-1, f} = \frac{P_i \left(y_i - \tan \varphi_c \left(0.5t_f - \frac{2I}{t_f^2} \right) \right) + 0.5W_i h_i \sin \psi_b - \frac{2I}{t_f} \left(\frac{\sigma_t}{F_s} + \frac{\cos \psi_b}{t_f} \right)}{y_{i-1} + \tan \varphi_c \left(0.5t_f - \frac{2I}{t_f^2} \right)} \tag{25}$$

in which,

σ_t : Tensile strength of blocks

I : Inertia moment

In Equation (25), P_i is applied from the block (I+1) to the block I. Since the block (I+1) can have the potential of sliding, toppling or stable, there are three states:

- If the block (I+1) has a prone to toppling failure, then $y_i = h_{i+1} - r$, and $P_i = P_{i,t}$

- If the block (I+1) has a prone to sliding failure, then $y_i = 0.5(h_{i+1} - r)$, and $P_i = P_{i,s}$

- If the block (I+1) is stable, then $P_i = 0$

b. The Ith block has the prone for shearing failure:

$$Q_i = P_i \tan \varphi_c \tag{26}$$

$$Q_{i-1} = P_{i-1} \tan \varphi_c \quad (27)$$

$$e = 0.5t_f \quad (28)$$

$$S_i = (c_i t_f + N_i \tan \phi_i) \quad (29)$$

$$y_{i-1} = 0.5(h_i - r) \quad (30)$$

In this case, the force P_{i-1} can also be determined by the limit equilibrium equation,

$$P_{i-1,sh} = P_i + \frac{W_i (\sin \psi_b - \cos \psi_b \tan \varphi_i / F_s) - c_i t_f / F_s}{1 - \tan \varphi_c \tan \varphi_i / F_s} \quad (31)$$

where:

ϕ_i : Interface friction angle in intact rock

c_i : Cohesive strength of intact rock

Finally, the value for P_{i-1} is equal to $P_{i-1} = \text{Max}(P_{i-1,f}, P_{i-1,sh}, 0)$.

In the limit equilibrium condition, $F_s = 1$. Using the above equation, the forces of inter-block can be calculated step by step for each column. Finally, by determining the sign of P_0 , the slope stability is evaluated against the block-flexural toppling of rock blocks with round corners, as follows: the slope is unstable when $P_0 > 0$; the slope is stable when $P_0 < 0$; and the slope is the state of limit condition when $P_0 = 0$. In order to determine the safety factor, P_0 is presumed to be 0, and the next F_s can be calculated by trial-and-error.

3. Assessment analysis of representative example

The suggested methodology was coded in a program that obtained the parameters of slope from the user and performed all calculation. A representative example was studied in order to evaluate the the proposed approach (as indicated in Figure 6). The results of this analysis are listed in Table 1. In the left and right sides of this Table, the outcomes of rectangular prismatic blocks and rounded edge blocks are displayed, respectively. In this example, the ratio of five curvature radius to the block thickness ($r/t = 0, 0.05, 0.1, 0.15, 0.2$) is analyzed. In this Table, the results of the rectangular prismatic blocks and rounded edge blocks ($r/t = 0.15$) are illustrated.

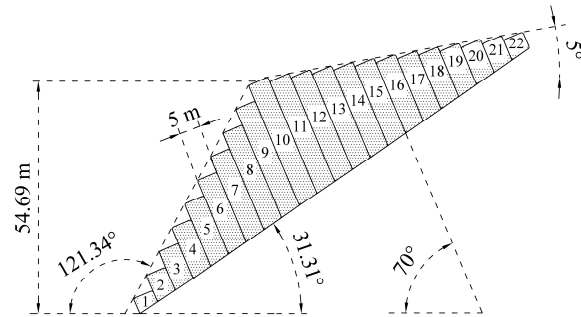
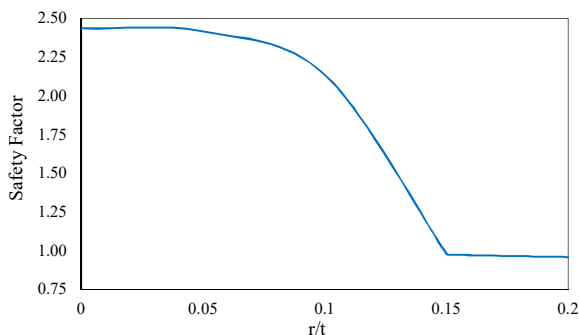


Figure 6. A representation diagram of the typical example.

According to the outcomes on the left side of this table, the blocks 17 to 22 are stable and the blocks 2 to 14 have the prone of block-flexural toppling failure. However, block 1 is stable ($P_0 < 0$), which indicates that this slope is stable, and F_s is equal to 2.44. As it can be seen on the right side of this Table, the blocks 19 to 22 are stable, and the blocks 1 to 14 have the prone to block-flexural toppling failure ($P_0 = 0.5MN$). Also the factor of safety value was obtained to be 0.98. The influence of the rounded block edges due to erosion is shown in Figure 7.

Table 1. Outcomes of analyzing the typical example.

Slope Geometry						
Column thickness (m)	Height of slope (m)	Number of blocks	Angle of face slope (Degree)	Angle of basal plane (Degree)	Block inclination (Degree)	Dip of normal to discontinuities (Degree)
5	54.69	22	58.66	31.31	70	20
Dip of upper surface (Degree)	Unit weight of blocks (KN/M ³)	Cohesive strength of blocks (MPa)	Tensile strength of intact blocks (MPa)	Friction angle of intact block (Degree)	Friction angle between blocks (Degree)	Friction angle block base (Degree)
5	28	20	2	35	28.5	35
Block-flexural toppling failure						
Rectangular prismatic blocks (r/thickness = 0)				Rounded edge blocks (r/thickness = 0.15)		
Column No.	Height (m)	Weight (MN)	Force (MN)	Failure mode	Force (MN)	Failure mode
22	2.42	0.34	0	stable	0	stable
21	4.76	0.67	0	stable	0	stable
20	7.10	0.99	0	stable	0	stable
19	9.44	1.32	0	stable	0	stable
18	11.78	1.65	0	stable	0.05	toppling
17	14.12	1.98	0	stable	0.00	stable
16	16.46	2.30	0.07	toppling	0.17	toppling
15	18.80	2.63	0.00	stable	0.06	flexural
14	21.14	2.96	0.18	toppling	0.31	toppling
13	23.48	3.29	0.33	flexural	0.48	flexural
12	25.82	3.61	0.49	toppling	0.69	toppling
11	28.16	3.94	0.92	flexural	1.15	flexural
10	30.50	4.27	1.14	toppling	1.42	toppling
9	27.50	3.85	2.00	flexural	2.41	flexural
8	24.50	3.43	1.86	toppling	2.29	toppling
7	21.50	3.01	2.75	flexural	3.39	flexural
6	18.50	2.59	2.31	toppling	2.93	toppling
5	15.50	2.17	3.09	flexural	4.04	flexural
4	12.50	1.75	2.47	toppling	3.36	toppling
3	9.50	1.33	2.78	flexural	4.30	flexural
2	6.50	0.91	2.32	sliding	3.90	toppling
1	3.50	0.49	0	stable	0.50	flexural

**Figure 7. Changes in the safety factor versus curvature radius to block thickness.**

4. Case study of rock slope facing Galandrood mine

This slope is situated in the north of Iran. The picture of this slope is shown in Figure 8. As it can be seen in this figure, the rock mass consists of limestone (sedimentary rock), some of the rock blocks have been broken, and a local instability is observed but no complete failure has occurred. The geometrical information and the kinematic analysis of this slope are indicated in Figure 9 and Figure . Based on these figures, it appears that the dominant failure is the flexural toppling failure. However, some cross-joints are also exhibited in the rock columns so that some rock blocks are susceptible to the block toppling failure [23].

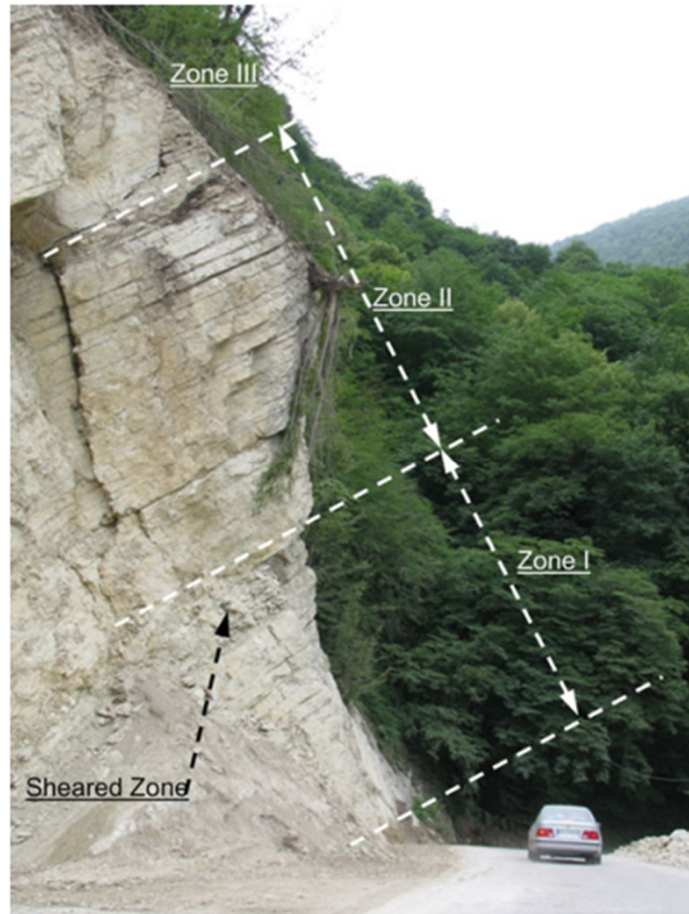


Figure 8. Rock slope facing Galandrood mine [23].

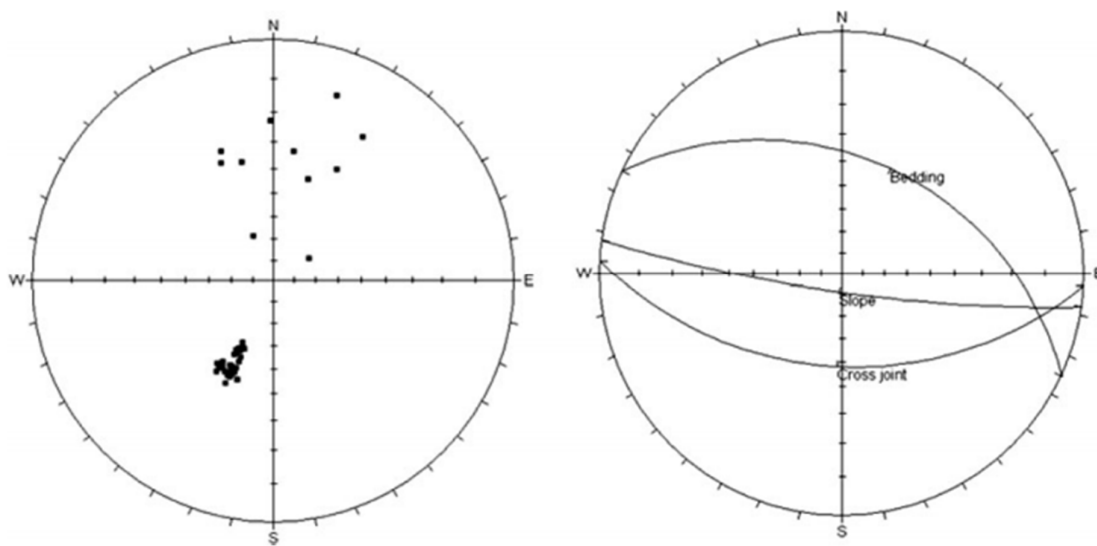


Figure 9. Stereonet figures of discontinuities [23].

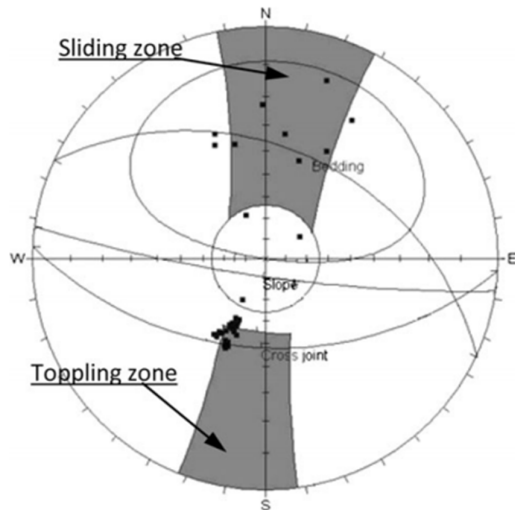


Figure 10. Kinematic stability analysis [23].

Amini *et al.* [23] have analyzed the stability of this slope for rectangular prismatic blocks, and calculated the value of the safety factor to be 1.38. The slope geometry and properties used in this problem have been gained from the study of Amini *et al.* [23]. If the impact of the erosion and block rounding edges is examined, this slope will be on the threshold of instability. In other words, the value of the safety factor approaches 1. The results of this analysis for $r/t = 0.11$ are presented in Table 2. The safety factor value of 1.14 was computed. As it can be seen in this table, there is a local failure in the blocks 71 to 93, and the blocks 5 to 69 have the potential of block-flexural toppling failure. At the toe part of the slope, only the blocks 1 and 2 are stable. Therefore, this slope can be unstable in the next few years.

Table 2. Results of analyzing of the Galandrood mine slope.

Slope Geometry						
Column thickness (m)	Height of slope (m)	Number of blocks	Angle of face slope (Degree)	Angle of basal plane (Degree)	Block inclination (Degree)	Dip of normal to discontinuities (Degree)
0.3	16.5	95	81	58	39	51
Dip of upper surface (Degree)	Unit weight of blocks (KN/M ³)	Cohesive strength of blocks (MPa)	Tensile strength of intact blocks (MPa)	Friction angle of intact block (Degree)	Friction angle between blocks (Degree)	Friction angle block base (Degree)
32	27	1.11	5	45	26	26

Block-flexural toppling failure for rounded edge blocks ($r/\text{thickness}=0.11$)

Column Number	Height (M)	Weight (KN)	Force (KN)	Failure Mode
95	0.04	0.32	0	stable
94	0.16	1.30	0	stable
93	0.30	2.43	0.38	toppling
92	0.44	3.56	0	stable
91	0.59	4.78	1.31	toppling
90	0.73	5.91	0	stable
89	0.87	7.05	2.20	toppling
88	1.01	8.18	0	stable
87	1.15	9.32	3.08	toppling
86	1.29	10.45	0	stable
85	1.43	11.58	3.96	toppling
84	1.57	12.72	0	stable
83	1.71	13.85	4.85	toppling
82	1.85	14.99	0	stable
81	1.99	16.12	6.01	sliding
80	2.13	17.25	0	stable
79	2.27	18.39	7.41	sliding
78	2.41	19.52	0	stable
77	2.55	20.66	8.81	sliding
76	2.69	21.79	0	stable
75	2.83	22.92	10.21	sliding
74	2.97	24.06	0	stable
73	3.11	25.19	11.61	sliding

Continu of Table 2

72	3.25	26.33	0	stable
71	3.39	27.46	13.01	sliding
70	3.53	28.59	0	stable
69	3.67	29.73	14.40	sliding
68	3.81	30.86	3.16	flexural
67	3.95	32.00	18.97	sliding
66	4.09	33.13	10.45	flexural
65	4.23	34.26	27.66	sliding
64	4.37	35.40	21.46	flexural
63	4.51	36.53	40.07	sliding
62	4.65	37.67	35.89	flexural
61	4.79	38.80	55.89	sliding
60	4.93	39.93	53.48	flexural
59	5.07	41.07	74.89	sliding
58	5.21	42.20	74.05	flexural
57	5.35	43.34	96.85	sliding
56	5.49	44.47	97.43	flexural
55	5.63	45.60	121.63	sliding
54	5.77	46.74	123.49	flexural
53	5.91	47.87	149.09	sliding
52	6.05	49.01	152.14	flexural
51	6.19	50.14	179.13	sliding
50	6.33	51.27	183.27	flexural
49	6.47	52.41	211.66	sliding
48	6.47	52.41	225.11	flexural
47	6.33	51.27	252.80	sliding
46	6.20	50.22	264.50	flexural
45	6.06	49.09	290.84	sliding
44	5.93	48.03	301.06	flexural
43	5.79	46.90	326.06	sliding
42	5.65	45.77	335.26	flexural
41	5.52	44.71	358.91	sliding
40	5.38	43.58	366.61	flexural
39	5.24	42.44	388.86	sliding
38	5.11	41.39	394.21	flexural
37	4.97	40.26	415.11	sliding
36	4.83	39.12	419.48	flexural
35	4.70	38.07	439.03	sliding
34	4.56	36.94	441.62	flexural
33	4.43	35.88	459.83	sliding
32	4.29	34.75	460.52	flexural
31	4.15	33.62	477.32	sliding
30	4.02	32.56	474.76	flexural
29	3.88	31.43	490.21	sliding
28	3.74	30.29	486.49	flexural
27	3.61	29.24	500.60	sliding
26	3.47	28.11	494.39	flexural
25	3.33	26.97	507.09	sliding
24	3.20	25.92	496.45	flexural
23	3.06	24.79	507.81	sliding
22	2.93	23.73	493.78	flexural
21	2.79	22.60	503.78	sliding
20	2.65	21.47	487.60	flexural
19	2.52	20.41	496.26	sliding
18	2.38	19.28	475.55	flexural
17	2.24	18.14	482.81	sliding
16	2.11	17.09	454.13	flexural

Continu of Table 2

15	1.97	15.96	460.04	sliding
14	1.83	14.82	426.19	flexural
13	1.70	13.77	430.75	sliding
12	1.56	12.64	387.06	flexural
11	1.43	11.58	390.27	sliding
10	1.29	10.45	332.33	flexural
9	1.15	9.32	334.14	sliding
8	1.02	8.26	249.92	flexural
7	0.88	7.13	250.38	sliding
6	0.74	5.99	125.32	flexural
5	0.61	4.94	124.43	sliding
4	0.47	3.81	0	stable
3	0.33	2.67	0.87	toppling
2	0.20	1.62	0	stable
1	0.06	0.49	0	stable

5. Conclusions

In this work, the block-flexural toppling failure with rounded edges was evaluated. Due to the brittleness of rocks and their irregular discontinuities, an ideal toppling failure (pure flexural or block toppling) does not often occur in the nature. Thus the block-flexural toppling failure is more commonly seen in the nature. Rounding of the rock block corners is a particular feature of spheroidal weathering. In the block toppling mode, due to the existence of cross-joints at the block base, the rounding edges also happen at the base of the block; however, in the flexural toppling mode, the rounding edges occur only at the upper corners of the block. In this paper, an analytical approach was recommended for the mentioned failure regarding the erosion phenomenon. As the manual computing of stability analysis is time-consuming, based on the methodology presented in this work, a program code was established in the Excel in order to simplify the stability investigation of this failure, as mentioned above. This code gets the rock slope specification from the user, and computes its stability. The recommended method was investigated via a typical example and a case study. The outcomes show that in the stable slopes, where the safety factor is close to 1, due to erosion, the slope is subjected to failure. Since the safety factor is reduced, by considering the rounding in the block, the suggested methodology is conservative in evaluating the block-flexural toppling failure, and this methodology can be applied to assess this failure.

Reference

- [1]. Ashby, J. (1971). Sliding and toppling modes of failure in models and jointed rock slopes, Imperial College, University of London.
- [2]. Erguvanli, K., and Goodman, R.E. (1972). Applications of models to engineering geology for rock excavations, *Bull. Assoc. Eng. Geol.*, 9 (8): 104
- [3]. Wyllie, D.C., Mah, C.W., and Hoek, E. (2004). *Rock slope engineering : civil and mining*. Spon Press.
- [4]. Alejano, L.R. Gómez-Márquez, I., and Martínez-Alegria, R. (2010). Analysis of a complex toppling-circular slope failure, *Eng. Geol.*, 114 (1-2): 93-104
- [5]. Amini, M., Ardestani, A., and Khosravi, M.H. (2017). Stability analysis of slide-toe-toppling failure, *Eng. Geol.*, 228: 82-96
- [6]. Amini, M. Sarfaraz, H., and Esmaeili, K. (2018). Stability analysis of slopes with a potential of slide-head-toppling failure, *Int. J. Rock Mech. Min. Sci.*, 112: 108-121
- [7]. Amini, M., and Ardestani, A. (2019). Stability analysis of the north-eastern slope of Daralou copper open pit mine against a secondary toppling failure, *Eng. Geol.*, 249: 89-101
- [8]. Alejano, L.R., Veiga, M., Pérez-Rey, I., Castro-Filgueira, U., Arzúa, J., and Castro-Caicedo, Á. J. (2019). Analysis of a complex slope failure in a granodiorite quarry bench, *Bull. Eng. Geol. Environ.*, 78 (2):1209-1224
- [9]. Sarfaraz, H., Khosravi, M. H., and Amini, M. (2019). Numerical Analysis of Slide-Head-Toppling Failure, *J. Min. Environment*, 10 (4): 1001–1011
- [10]. Sarfaraz, H., and Amini, M. (2020). Numerical Simulation of Slide-Toe-Toppling Failure Using Distinct Element Method and Finite Element Method, *Geotech. Geol. Eng.*, 38 (2): 2199-2212
- [11]. Haghgoei, H., Kargar, A. R., Amini, M., and Esmaeili, K. (2020). An analytical solution for analysis of toppling-slumping failure in rock slopes, *Eng. Geol.*, 265: 105396
- [12]. Sarfaraz, H. (2020). A simple theoretical approach for analysis of slide-toe-toppling failure, *J. Cent. South*

Univ. Technol, 27 (9): 2745-2753

[13]. Alejano, L. R., Carranza-Torres, C., Giani, G. P., and Arzúa, J. (2015). Study of the stability against toppling of rock blocks with rounded edges based on analytical and experimental approaches, *Eng. Geol.*, 195: 172–184

[14]. Bobet, A. (2002). Analytical solutions for toppling failure, *Int. J. Rock Mech. Min. Sci.*, 36 (7): 971-980

[15]. Brideau, M. A., and Stead, D. (2010). Controls on block toppling using a three-dimensional distinct element approach, *Rock Mech. Rock Eng.*, 43 (3): 241–260

[16]. Babiker, A. F. A., Smith, C. C., Gilbert, M., and Ashby, J. P. (2014). Non-associative limit analysis of the toppling-sliding failure of rock slopes, *Int. J. Rock Mech. Min. Sci.*, 71: 1–11

[17]. Adhikary, D. P., and Dyskin, A. V. (2007). Modelling of progressive and instantaneous failures of foliated rock slopes, *Rock Mech. Rock Eng.*, 40 (4): 349–362

[18]. Amini, M., Majdi, A., and Aydan, Ö. (2009). Stability Analysis and the Stabilisation of Flexural Toppling Failure. *Rock Mech. Rock Eng.*, 42 (5): 751–782

[19]. Majdi, A., and Amini, M. (2011). Analysis of geo-structural defects in flexural toppling failure, *Int. J. Rock Mech. Min. Sci.*, 48 (2): 175–186

[20]. Zheng, Y., Chen, C., Liu, T., Zhang, H., Xia, K., and Liu, F. (2018). Study on the mechanisms of flexural toppling failure in anti-inclined rock slopes using numerical and limit equilibrium models, *Eng. Geol.*, 237: 116–128

[21]. Zheng, Y., Chen, C., Liu, T., Xia, K., and Liu, X.

(2018). Stability analysis of rock slopes against sliding or flexural-toppling failure, *Bull. Eng. Geol. Environ.*, 77 (4): 1383–1403

[22]. Sarfaraz, H. (2020). Stability Analysis of Flexural Toppling Failure Using the Sarma's Method, *Geotech. Geol. Eng.*, 38 (4): 3667–3682

[23]. Amini, M., Majdi, A., and Veshadi, M. A. (2012). Stability analysis of rock slopes against block-flexure toppling failure, *Rock Mech. Rock Eng.*, 45 (4): 519–532

[24]. Sarfaraz, H., and Amini, M. (2020). Numerical modeling of rock slopes with a potential of block-flexural toppling failure, *J. Min. Environ.*, 11 (1): 247–259

[25]. Zhang, Z., Wang, T., Wu, S., and Tang, H. (2016). Rock toppling failure mode influenced by local response to earthquakes, *Bull. Eng. Geol. Environ.*, 75 (4): 1361–1375

[26]. Qi Li, L., Pan Ju, N., Zhang, S., and Xue Deng, X. (2019). Shaking table test to assess seismic response differences between steep bedding and toppling rock slopes, *Bull. Eng. Geol. Environ.*, 78 (1): 519–531

[27]. Bowa, V. M., and Xia, Y. (2019). Influence of counter-tilted failure surface angle on the stability of rock slopes subjected to block toppling failure mechanisms, *Bull. Eng. Geol. Environ.*, 78 (4): 2535–2550

[28]. Alejano, L.R., Sánchez-Alonso, C., Pérez-Rey, I., Arzúa, J., Alonso, E., González, J., Beltramone, L., Ferrero, A.M. (2018). Block toppling stability in the case of rock blocks with rounded edges, *Eng. Geol.*, 234: 192–203

تحلیل پایداری شکست واژگونی بلوکی-خمشی با گرد شدگی در لبه‌های بلوک سنگی

حسن سرفراز*

دانشکده مهندسی معدن، پردیس دانشکده‌های فنی دانشگاه تهران، تهران، ایران

ارسال ۲۰۲۰/۱۰/۰۲، پذیرش ۲۰۲۰/۱۱/۲۵

* نویسنده مسئول مکاتبات: sarfaraz@ut.ac.ir

چکیده:

یکی از رایج‌ترین شکست‌های واژگونی، شکست واژگونی بلوکی-خمشی است که در پروژه‌های مهندسی عمران و معدن رخ می‌دهد. در این شکست، بعضی از بلوک‌ها در اثر خمش شکسته شده و برخی دیگر آزادانه حول پاشنه خود می‌چرخند و در نهایت همه آن‌ها با یکدیگر واژگون می‌شوند. ویژگی خاص هوازگی کروی، گرد شدن لبه‌های بلوک سنگی است. در حالت شکست واژگونی خمشی، گرد شدگی در لبه‌ها فقط در گوشه‌های بلوک اتفاق می‌افتد در حالی که در حالت شکست واژگونی بلوکی، به دلیل وجود درزه متعامد در پاشنه بلوک، گرد شدگی لبه‌ها در پایه بلوک نیز رخ می‌دهد. در این تحقیق، روش تحلیلی برای شکست واژگونی بلوکی-خمشی با گرد شدگی در لبه‌ها ارائه شده است. روش پیشنهادی از طریق مثال و مطالعه موردی مورد ارزیابی قرار گرفته است. نتایج این تحقیق نشان می‌دهد که شیروانی‌های پایدار با بلوک‌های مستطیلی شکل (بدون گرد شدگی در لبه) که مقدار فاکتور ایمنی نزدیک به یک باشد، به دلیل فرسایش، شیروانی ممکن است در آستانه ناپایداری قرار گیرد. همچنین نتایج بدست آمده نشان می‌دهد که روش تحلیلی پیشنهادی در تحلیل پایداری شکست واژگونی بلوکی-خمشی محافظه کارانه است و می‌توان از این روش برای ارزیابی این شکست استفاده کرد.

کلمات کلیدی: تحلیل پایداری شیروانی‌های سنگی، هوازگی کروی، گرد شدگی در لبه، روش تحلیلی
